AIR 5021 Project

Yuanchen Tang Yan Lin
Zhenkun Huo
The Chinese University of Hongkong,Shenzhen

May 2025

1 Introduction

In the field of humanoid robotics, particularly in the control of robotic arms, the fully-actuated system approach[1][2][3] is gaining increasing attention and application from researchers[4][5][6]. This method stands out for its excellent trajectory tracking accuracy[7] and strong nonlinear processing capabilities[8][9]. The fully-actuated system approach requires the design of a non-linear disturbance observer[10] and a state feedback controllers[11]. Through the designed observer, the nonlinear terms of the system can be precisely observed; the state feedback controller is responsible for adjusting the system's eigenvalues[13]. Ultimately, the observed nonlinear terms and the controller's output are compensated back into the original system, transforming it into a system with the desired characteristics[13][14]. Compared to traditional feedback linearization methods, the fully-actuated system approach does not reduce the order of the system[15][16], effectively avoiding the potential destruction of the original physical properties of the system during the feedback linearization process[17][18]. For robotic arms, the fully-actuated system method involves: 1.High-order dynamic modeling to retain the intrinsic physical properties of the multi-joint system. 2.Nonlinear disturbance observers to decouple and estimate interactions between joints. 3.State feedback controllers to dynamically assign eigenvalues for each DoF. This study focuses on applying the high-order fully-actuated approach to robotic arms, aiming to demonstrate its superiority in trajectory tracking for pick-and-drop tasks.

2 Preliminary

2.1 Dynamic Modeling

The robot platform studied in this paper is a 6-DOF robotic arm. In the frame $\{j\}$, the center of mass of rod i can be expressed as ${}^{j}c_i$. The center of mass of rod i in frame $\{0\}$ (ground) can be expressed below.

$$^{0}c_i =_{j}^{0} T^{j} c_i \tag{1}$$

where, ${}_{j}^{0}T$ is the transformation matrix between frame $\{0\}$ and frame $\{j\}$.
The linear velocity of the center of mass of each rods can be obtained as follows:

$$v_{c_i} = \frac{d(^{0}c_i)}{dt} \tag{2}$$

The angular velocity can be expressed as:

$$^{i+1}w_{i+1} =^{i} w_i + (\theta_{i+1})^{i+1} Z_{i+1} \tag{3}$$

where $^{i+1}Z_{i+1}$is the positive direction of the rotation axis of joint $i+1$. $^{i}w_i$ represents the angular velocity of rod i in frame $\{i\}$. is the the angular velocity of rod $i+1$. In the process of the connecting rod rotating around the center of mass, its inertia tensor can be expressed as:

$$^{c_i}I_i = \begin{pmatrix} I_{xx} & I_{xy} & I_{xz} \\ I_{yx} & I_{yy} & I_{yz} \\ I_{xz} & I_{yz} & I_{zz} \end{pmatrix} \tag{4}$$

In the matrix, the diagonal element is the mass moment of inertia of the rigid body about the coordinate axis, and the remaining elements are the product of inertia. In order to simplify the Lagrangian dynamics calculation, we only take the elements in the principal diagonal of the inertia tensor for calculation. The kinetic energy of the system is the of translation energy and rotation energy:

$$E_K = E_{translate} + E_{rotate} \tag{5}$$

$$E_{translate} = \sum_{6}^{i=1} \frac{1}{2} m_i v_{c_i}^{T} v_{c_i} \tag{6}$$

$$E_{rotate} = \sum_{6}^{i=1} \frac{1}{2} {}^{i}w_i^{T\,c_i} I_i {}^{i}w_i \tag{7}$$

The potential energy of the system can be expressed as:

$$E_P = \sum_{6}^{i=1} m_i g {}^{0}y_{c_i} \tag{8}$$

where$^{0}y_{c_i}$ is the height of the center of mass of rod i in frame$\{0\}$ (ground). The Lagrangian dynamic equation can be expressed as:

$$\frac{d}{dt}\frac{\partial L}{\partial \dot{\theta}} - \frac{\partial L}{\partial \theta} = u \tag{9}$$

where, Lagrange function $L = E_k - E_P$, is the joint angle, and u is the output torque of the controller. After calculation, the 6-DOF Lagrangian dynamic equation can be obtained as follows:

$$M(\theta)\ddot{\theta} + D(\theta, \dot{\theta})\dot{\theta} + G(\theta) = u \tag{10}$$

where $M(\theta)$ is a 6×6 mass matrix, $D(\theta, \dot{\theta})$ is a 6×6 Coriolis force and centripetal force matrix, $G(\theta)$ is a 6×1 gravity vector, and u is a 6×1 torque vector.

2.2 Standard form of a second-order fully-actuated system approach

The standard form of the second-order fully-actuated system equation is:

$$M(\theta, x, \dot{x})\ddot{x} + D(\theta, x, \dot{x})\dot{x} + K(\theta, x, \dot{x})x + \xi(\theta, x, \dot{x}) = B(\theta, x, \dot{x})u \tag{11}$$

where vector $x \in R^{n\times1}$ is the state vector of the system, vector $u \in R^{n\times1}$ is the control vector of the system, and vector $\xi(\theta, x, \dot{x})$ is a piecewise continuous vector $\theta = \theta(t) \in R^{l\times1}$ is the parameter vector. $M(\theta, x, \dot{x})\ddot{x}, D(\theta, x, \dot{x})\dot{x}, K(\theta, x, \dot{x}), B(\theta, x, \dot{x}) \in R^{n\times n}$ is the coefficient matrix of the second-order fully-actuated system equation. The second-order fully-actuated system approach is based on constraints 1-3:
Constraint 1. A parameter vector $\theta = \theta(t)$ is contained in some compact set Ω .
Constraint 2. $|B| \neq 0$,$\forall x$,$\dot{x}$ and $\theta(t) \in \Omega$.
Constraint 3. $|M| \neq 0$,$\forall x$,$\dot{x}$ and $\theta(t) \in \Omega$.
The error dynamics equation of robotic arm can be expressed as:

$$M(\theta_e)\ddot{\theta_e} + D(\theta_e, \ddot{\theta_e})\dot{\theta_e} + G(\theta_e) = u + d \tag{12}$$

where,$\theta_e = \theta_r + \theta_d$. $\theta_r$represents the error of each joints, $\theta_d$represents the actual output of each joints and d represents the target tracking function of each joints. is the non-linear term of the system.

3 Controller Design

It's obviously that the 6-DOF robotic arm studied in this paper is fully-actuated. Based on this, we can design the controller based on fully-actuated system approach. The controller can be expressed as:

$$u = u_c + u_f \tag{13}$$

where, u_c is a non-linear disturbance observer and u_f is a state feedback controller.

3.1 Nonlinear Disturbance Observer Design

An improved observer can be expressed as:

$$\begin{cases} z = \hat{d} - p \\ \dot{z} = -Lz + L(d\dot{q_e} + G - u - p) \\ p = m_p \times \dot{q}_e \\ L = m_p M^{-1} \end{cases}$$

where $\hat{d}$, is the estimate value of the non-linear term d. z ,L ,P are intermediate vectors. $m_p$can be expressed as:

$$m_p = \begin{bmatrix} c_1 & 0 & 0 & 0 & 0 & 0 \\ 0 & c_2 & 0 & 0 & 0 & 0 \\ 0 & 0 & c_3 & 0 & 0 & 0 \\ 0 & 0 & 0 & c_4 & 0 & 0 \\ 0 & 0 & 0 & 0 & c_5 & 0 \\ 0 & 0 & 0 & 0 & 0 & c_6 \end{bmatrix}$$

The non-linear disturbance observer is asymptotically stable when the following conditions are met:

$$\begin{cases} M(q_e) = m_p^T M(\bar{q_e}) m_p \\ \tilde{M} = 2(m_p^T)^{-1} - \frac{d\bar{M}}{dt} \\ \left|\tilde{M}\right| > 0 \end{cases}$$

3.2 State Feedback Controller Design

The state feedback controller can be expressed as:

$$u_f = K_0\theta_e + K_1\dot{\theta_e} + B^{-1}G + \nu \tag{14}$$

where, $B^{-}1 = I_2 \in R^{6\times6}$. $K_0 \in R^{6\times6}$ and $K_1 \in R^{6\times6}$ are the feedback matrix need to be obtained.

The following steps is to obtain matrix K_0 and K_1 :

Step 1. Construct matrix F and Z

$$\begin{cases} F \in R^{12\times12} \\ \lambda_i(F) \in C^-, i = 1, 2, 3, \ldots, 12 \\ Z \in R^{6\times12} \\ \begin{vmatrix} Z \\ ZF \end{vmatrix} \neq 0 \end{cases}$$

where, the eigenvalue matrix F is a 12×12 diagonal matrix whose principal diagonal values are the linear time-invariant system's eigenvalue in equation (14). To ensure that a linear time-invariant system can converge, we take all elements of the principal diagonal of F in the left half plane.

Step 2. Calculate matrix K_0 and K_1

$$\begin{cases} V = \begin{vmatrix} Z \\ ZF \end{vmatrix} \\ W = B^{-1}(MZF^2 + DZF) \\ F = V^{-1}A_cV \\ [K_0, K_1] = WV^{-1} \end{cases}$$

4 Experiment

4.1 Simulation Environment and platform

The experimental validation of the proposed fully-actuated control approach was conducted in MATLAB, leveraging its high-fidelity multibody dynamics and control system toolboxes. The robotic arm was modeled as a 6-DOF serial manipulator as $sagittarius_arm$ using the Denavit-Hartenberg (DH) convention, with parameters adjusted to replicate the kinematic and dynamic properties of it. Here's the DH table we model:

4.2 Experimental Design

First of all, we will initiate the parameters of the observer and feedback controller by some experiment sense. m_p from disturbance observer will be initialize as follow:

$$m_p = \begin{bmatrix} 25 & 0 & 0 & 0 & 0 & 0 \\ 0 & 20 & 0 & 0 & 0 & 0 \\ 0 & 0 & 15 & 0 & 0 & 0 \\ 0 & 0 & 0 & 5 & 0 & 0 \\ 0 & 0 & 0 & 0 & 1 & 0 \\ 0 & 0 & 0 & 0 & 0 & 0.1 \end{bmatrix} \quad c = 1$$

F and Z from the state feed back controller design will be initialize as follow:

$$F = \begin{bmatrix} P_1 & 0 & 0 & \dots & 0 \\ 0 & P_2 & 0 & \dots & 0 \\ 0 & 0 & P_3 & \dots & 0 \\ \vdots & \vdots & \vdots & & \vdots \\ 0 & 0 & 0 & \dots & P_{12} \end{bmatrix} \quad Z = \begin{bmatrix} 2I_{6\times6} & I_{6\times6} \end{bmatrix}$$

where:

$$\begin{cases} P_1 = -5, P_7 = -30 \\ P_2 = -5, P_8 = -30 \\ P_3 = -5, P_9 = -30 \\ P_4 = -5, P_{10} = -15 \\ P_5 = -5, P_{11} = -35 \\ P_6 = -5, P_{12} = -35 \end{cases}$$

and $I_{6\times6}$ is the identity matrix.

These setting will satisfy the condition of both observer and feedback controller, which ensures the system stablity.
Now we can conduct the experiment on it.
The experiment will conduct following two parts:
Trajectory Tracking Task:
The model was tasked with tracking a predefined sin waves with nonlinear features. In the process, the output torque and pose of all joints will be generated as the result. Evaluation:
To evaluate the performance of our approach, we would record the tracking error of the system and compare our system with PD and backstepping method.

4.3 Result

In this session, we will present the result as two sets. The first set shows our system tracking signal compare to the real siganl. The second set shows the comparison between our system and PD,backstepping.

4.3.1 Tracking result of fully-acutated system

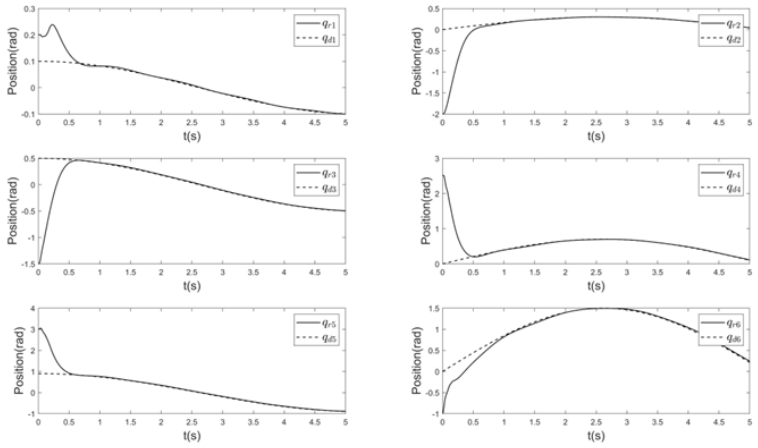

Figure 1

Figure 1 and 2 shows the tracking result of our system and the real arm for all joints in pose and amplitude. Figure 3 shows the tracking error of our system in term of joint position.
As clearly demonstrated in Figures 1 and 2, the proposed control system exhibits excellent signal acquisition capabilities and tracking performance. The system's response closely matches the reference trajectory with high precision, achieving near-perfect alignment with the desired motion profile. Notably, after just a few operational iterations, the controller demonstrates remarkable adaptation,

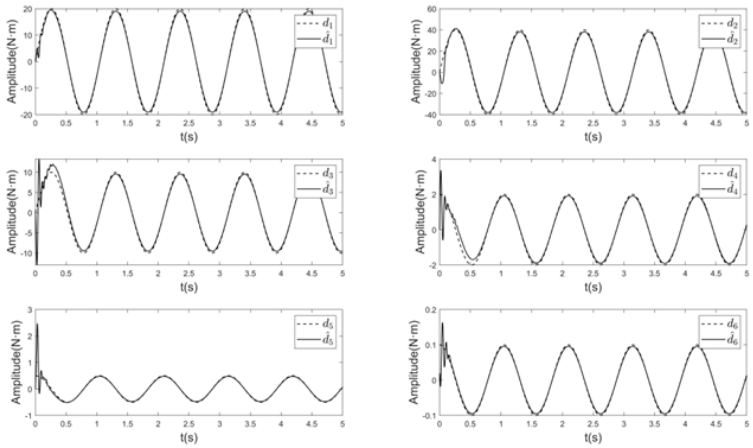

Figure 2

producing joint movements that are virtually indistinguishable from those of the actual robotic arm system in both pose and amplitude.
Figure 3 also provides further validation of the system's superior control capabilities. The tracking error exhibits rapid asymptotic convergence, reaching and maintaining a near-zero steady-state value. This robust convergence behavior persists even during dynamic trajectory changes, conclusively verifying the effectiveness of our fully-actuated control architecture.

4.3.2 Disturbance

Figure 5 shows the error between the actual disturbance of the sin waves and the disturbance our observer observed.
As evidenced in Figure 5, the proposed nonlinear disturbance observer demonstrates exceptional performance in estimating and tracking the actual sinusoidal disturbances introduced to the system. The observed disturbance signal closely follows the reference disturbance profile, with the error between the two converging rapidly. This precise estimation holds consistently across multiple disturbance cycles, confirming the observer's robustness to periodic nonlinearities.

4.3.3 Fully-actuted system output

Figure 6,7,8 sequantially show the output torque of six joints respect to the obsever, state-feedback controller and the whole fully-actuated system. The nonlinear disturbance observer generates smooth, anticipatory torque signals that Proactively counteract disturbance patterns.
The eigenvalue-optimized feedback controller demonstrates that precisely scaled torque amplitudes matching inertial requirements.

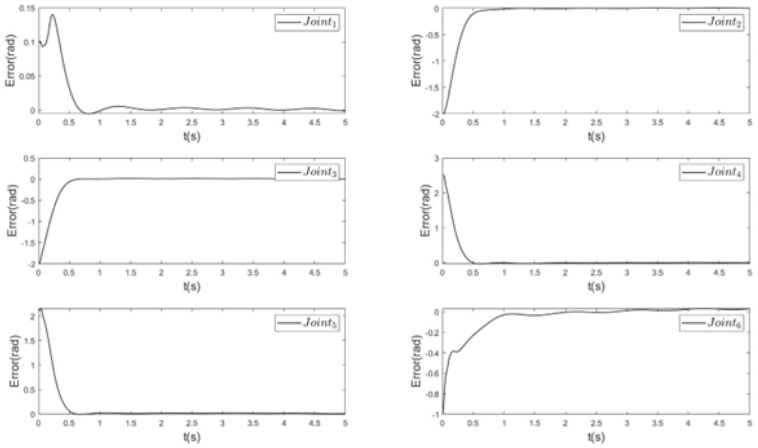

Figure 3

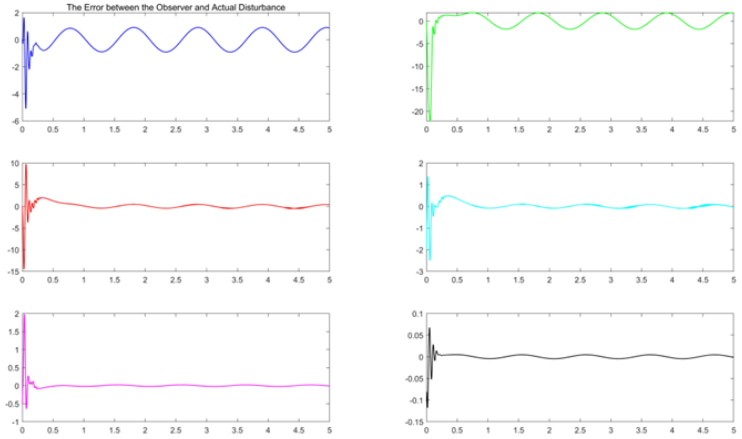

Figure 4: The error between the actual disturbance and the observer obtained

The integrated System output reveals that Observer handles nonlinear compensation while feedback controller provides primary trajectory tracking.

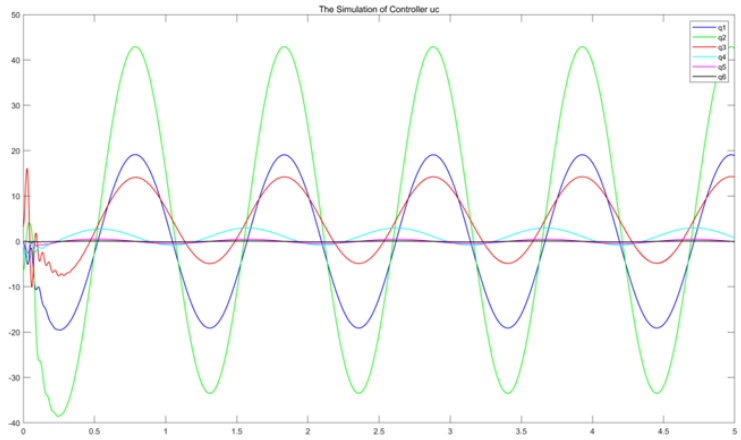

Figure 5

4.3.4 Comparison Result

Figure 8 shows the comparison between fully-actuated system and PD,Backsteeping method.

The experimental results clearly demonstrate the fundamental limitations of conventional PD control in handling the robotic arm's nonlinear dynamics. As shown in the tracking plots, the PD controller fails to compensate for nonlinear effects.
While the backstepping shows improved nonlinear handling capability, our system achieves superior performance through precision tracking with lower tracking error and transient Performance that settling time shortened by 50% in the tracking process.

5 Future Works

While the proposed fully-actuated control system demonstrates superior performance in simulation, several practical challenges must be addressed for real-world deployment on physical robotic arms:
1.real-Time Computation Constraints:
The proposed fully-actuated control system relies on computationally intensive operations, including real-time matrix inversion for the disturbance observer and eigenvalue assignment for the state feedback controller. While feasible in

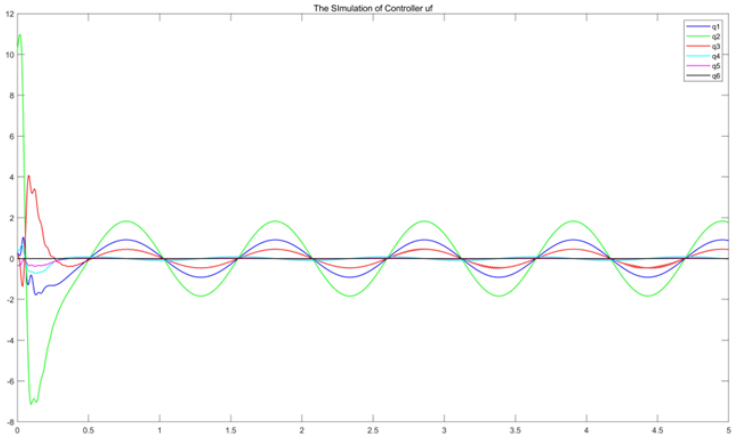

Figure 6

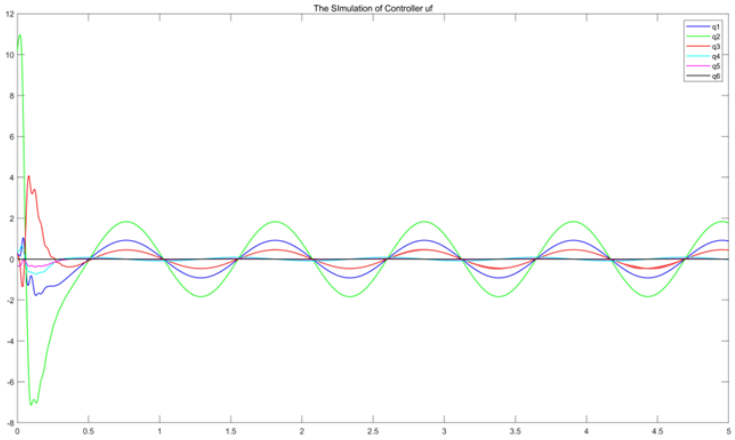

Figure 7

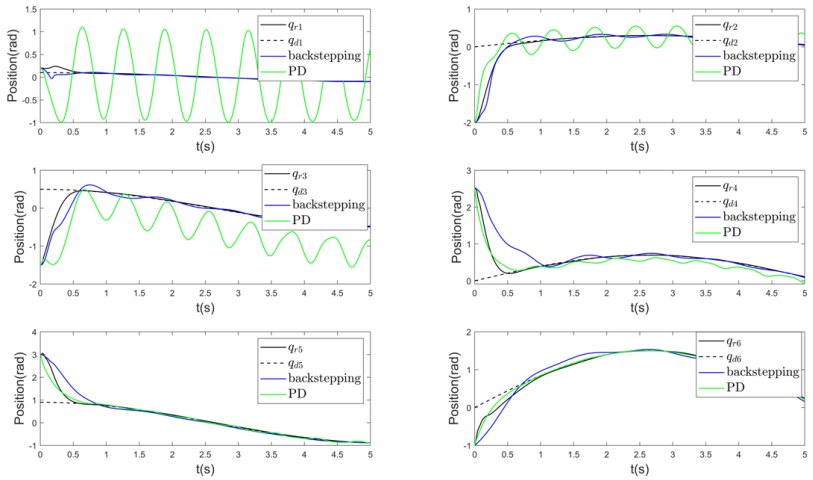

Figure 8: Comparison between our system and PD,Backstepping

simulation, these calculations may exceed the processing capabilities of standard robotic control hardware operating at high frequencies (e.g., 1 kHz). Latency in solving these equations could degrade system performance, particularly during dynamic maneuvers requiring rapid torque updates. 2.Hardware Control Layer Limitations Modern robotic arms often abstract low-level torque control behind proprietary motion planning interfaces. Although our system calculates precise joint torque commands, many industrial platforms (e.g. ROS) only accept position/velocity inputs, preventing direct torque application. This forces an additional control layer (e.g., impedance control), which may dilute the benefits of our method's exact nonlinear compensation.

In future, we may try integrating the following two steps to solve the challenge.

1.Real-Time Optimization

Algorithm Refinement: Replace matrix inversion with iterative solvers (e.g., Jacobi method) or precomputed lookup tables for critical operations.

Hardware Acceleration: Deploy the controller on FPGA or GPU-embedded systems (e.g., NVIDIA Jetson) to meet timing constraints.

Edge Computing: Offload state estimation to a co-processor while maintaining high-frequency torque control on the main CPU.

2.Torque Control Integration

Middleware Development: Create a ROS 2/Industrial API bridge to map our torque outputs to vendor-specific interfaces.

Collaborative Robot Targeting: Prioritize platforms with open torque control APIs.

Hybrid Position-Torque Mode: Implement hierarchical control where our method handles fine torque adjustments atop the robot's native motion planner.

6 Conclusion

This paper presented a fully-actuated control system for high-performance robotic arm manipulation, combining a nonlinear disturbance observer with eigenvalue-optimized state feedback. Through MATLAB/Simulink simulations, the proposed method demonstrated superior trajectory tracking accuracy,faster convergence ability and robust disturbance rejection compared to conventional PD and backstepping controllers.

Key innovation is the physics-preserving design that the fully-actuated formulation maintains system order while enabling exact nonlinear compensation. Current limitations in real-time computation and industrial deployment pathways point to critical next steps: Embedded Implementation: Porting to GPU/FPGA platforms for μ s-level latency

Vendor Integration: Developing middleware for torque control on collaborative robots

These advances will transition the method from simulation to real-world applications requiring precision force-motion control, such as compliant assembly or human-robot collaboration. The results establish a new benchmark for model-based control in robotic manipulation, bridging theoretical rigor with practical deployability.

A Github Repository

The code is on the following github repository
`https://github.com/SocialTigerBro/CUHK-Shenzhen-AIR5021-Team10`

References

[1] G. Duan, "High-order System Approaches: I. Fully-actuated Systems and Parametric Designs," *Acta Automatica Sinica*, vol. 46, no. 7, pp. 1333–1345, 2020.

[2] G. Duan, "High-order fully actuated system approaches: Part II. Generalized strict-feedback systems," *International Journal of Systems Science*, vol. 52, no. 3, pp. 437–454, 2021.

[3] G. Duan, "High-order System Approaches: III. Observability and Observer design," *Acta Automatica Sinica*, vol. 46, no. 9, pp. 1885–1895, 2020.

[4] M. Zhang, Z. Zhou, N. Sun, H. Geng, J. Zhao, and Z. Yang, "Bioinspired Reference Model and Fully Actuated System Approach-Based Neuroadaptive Control for Uncertain Active Suspension Systems With Input Dead Zones," *IEEE Transactions on Industrial Electronics*, 2025, doi: 10.1109/TIE.2025.3536552.

[5] H. Sun, L. Huang, and L. He, "Research on the Trajectory Tracking Control of a 6-DOF Manipulator Based on Fully-Actuated System Models," *Journal of Systems Science and Complexity*, vol. 35, pp. 641–659, 2022.

[6] G. Tian, J. Tan, B. Li, and G. Duan, "Optimal Fully Actuated System Approach-Based Trajectory Tracking Control for Robot Manipulators," *IEEE Transactions on Cybernetics*, vol. 54, no. 12, pp. 7469–7478, 2024.

[7] Q. Pan, X. Peng, and X. Wang, "Stabilization Control of Second-order Nonholonomic System with High-Order Fully Actuated System Approach," in *Proc. 2024 3rd Conference on Fully Actuated System Theory and Applications (FASTA)*, Shenzhen, China, 2024, pp. 1072–1077.

[8] X. Zou, H.-J. Sun, D. Meng, T. Guo, and B. Liang, "Practical Prescribed-Time Trajectory Tracking Control for a Novel Tendon-Driven Space Manipulator via Fully Actuated System Approaches," *IEEE/ASME Transactions on Mechatronics*, 2025, doi: 10.1109/TMECH.2025.3528990.

[9] Y. Lu, K. Zhang, and B. Jiang, "Fully Actuated System Approach Based Prescribed-Time Fault-Tolerant Formation Control for Unmanned Helicopters Under Fixed and Switching Topologies," *IEEE Transactions on Circuits and Systems I: Regular Papers*, vol. 71, no. 11, pp. 5249–5260, 2024.

[10] F. Yao, G. Tian, A. Wu, G.-R. Duan, and H. Kong, "A High-Order Fully Actuated System Approach to Control of Overhead Cranes," *IEEE/ASME Transactions on Mechatronics*, 2024, doi: 10.1109/TMECH.2024.3446670.

[11] Q. Huang, J. Sun, and C. Zhang, "High-Order Fully Actuated System Approach to Robust Control of Impulsive Systems," *IEEE Transactions on Circuits and Systems II: Express Briefs*, vol. 71, no. 3, pp. 1321–1325, 2024.

[12] Y. Wang, G. Duan, and P. Li, "Event-Triggered Adaptive Control of Uncertain Strict-Feedback Nonlinear Systems Using Fully Actuated System Approach," *IEEE Transactions on Cybernetics*, vol. 54, no. 11, pp. 6371–6383, 2024.

[13] C. Yan, J. Xia, J. H. Park, J.-e. Feng, and X. Xie, "Fully Actuated System Approach-Based Dynamic Event-Triggered Control With Guaranteed Transient Performance of Flexible-Joint Robot: Experiment," *IEEE Transactions on Circuits and Systems II: Express Briefs*, vol. 71, no. 8, pp. 3775–3779, 2024.

[14] G.-Q. Duan, G.-P. Liu, and Y.-M. Fu, "Combined Spacecraft Attitude Tracking Control with Prescribed Performance via A Fully Actuated System Approach," in *Proc. 2023 42nd Chinese Control Conference (CCC)*, Tianjin, China, 2023, pp. 5253–5257.

[15] H. Jiang, Y. Yang, C. Hua, X. Li, and F. Lu, "Predefined-Time Composite Fuzzy Adaptive Control for Flexible-Joint Manipulator System With High-Order Fully Actuated Control Approach," *IEEE Transactions on Industrial Electronics*, 2024, doi: 10.1109/TIE.2024.3515255.

[16] Z. Mo, W. Liu, Y.-Y. Wu, and H.-J. Sun, "Fully Actuated Behavioral Control for Multiple Omnidirectional Mobile Robots System with Uncertain Dynamics," in *Proc. 2024 3rd Conference on Fully Actuated System Theory and Applications (FASTA)*, Shenzhen, China, 2024, pp. 189–194.

[17] S. Lu, K. Tsakalis, and Y. Chen, "Development and Application of a Novel High-Order Fully Actuated System Approach—Part I: 3-DOF Quadrotor Control," *IEEE Control Systems Letters*, vol. 7, pp. 1177–1182, 2023.

[18] Y. Huang, G.-P. Liu, Y. Yu, and W. Hu, "Constrained Networked Predictive Control for Nonlinear Systems Using a High-Order Fully Actuated System Approach," *IEEE/CAA Journal of Automatica Sinica*, vol. 12, no. 2, pp. 478–480, 2023.